This is the accepted manuscript version of the conference paper: Cantù, E., Tonello, S., Serpelloni, M., Sardini, E. (2019). Aerosol Jet Printed Sensors for Protein Detection: A Preliminary Study. In: Andò, B., *et al.* Sensors. CNS 2018. Lecture Notes in Electrical Engineering, vol 539. Springer, Cham. https://doi.org/10.1007/978-3-030-04324-7_40.
The final published version and copyright permissions are available on https://link.springer.com/chapter/10.1007/978-3-030-04324-7_40

Aerosol Jet Printed Sensors for Protein Detection: a preliminary study

Edoardo Cantù, Sarah Tonello, Mauro Serpelloni and Emilio Sardini

Department of Information Engineering, University of Brescia,
Via Branze, 38 - 25123 Brescia,
s.tonello@unibs.it

Abstract. The possibility to implement engineered devices to obtain feedbacks from biological samples is taking diagnostics and biotechnological research to a new level. Aerosol Jet Printing (AJP) represents a promising technique for this kind of applications. The benefits are related to manufacturing of customized, complex geometries with a high resolution even on irregular surfaces without masks. In this paper, we present the realization of an Aerosol Jet Printed micro-device addressed to protein detection and quantification in biological samples. The sensor was realized with particular attention to materials and geometry choices. The thickness of printed layers was measured thanks to a profilometer, while electric tests were performed thanks to a multimeter, in order to evaluate the electrical resistance offered by the printed elements. Finally, the possibility to immobilize antibodies on sensor surface for electrochemical protein quantification was assessed with fluorescence imaging. Final results obtained stated the possibility to print with AJP high resolution lines, with proper values of resistivity. Imaging findings showed a good adhesion of antibodies on the electrodes, Ag-based Anodic stripping voltammetry confirmed sensors' capability to quantify proteins, proposing the designed sensors as promising for the analysis of real biological samples.

Keywords: microsensor; protein detection; 3-D printing; aerosol jet printing

1 Introduction

1.1 Introduction

Printed electronics has emerging as promising candidate in fields like diagnostics or tissue engineering with technological platforms giving feedbacks on biological samples or physiological processes. Moreover, the recent attention for disposable, low-cost and reliable biomolecule-to-chip interface systems for high-throughput in-vitro toxicity assays and pharmacology, is becoming a urgent need due to novel international regulatory guidelines [1].

Methods such as screen printing or ink-jet printing are most frequently selected for these applications: electrochemical sensors for biotechnological applications produced with these techniques range from chemicals detection to DNA or protein recognition

[2], [3]. These two techniques have been also combined, in order to detect ascorbic acid with a disposable paper-based electrochemical sensor fabricated using screen-printing for base material and inkjet-printing for modifying functional material [4]. Inkjet printing was also employed to develop a method to fabricate hundreds of nano-porous gold electrode arrays on cellulose membranes for electrochemical oxygen sensing, using ionic liquid (IL) electrolytes [5].

Despite the cost and time effectiveness of these technique, they present some issues in term of reproducibility, resolution and difficulty to realize 3D structures useful for a proper management of liquid samples.

In this picture, the possibility to improve resolution, customization, standardization, and to realize complex customized 3D structures makes additive manufacturing a promising potential candidate to bring the production of biosensors to a next level [6], [7]. AM represents a process of joining materials to make objects from 3D model data, usually layer upon layer, following the definition given by the American Society for Testing Materials (ASTM) International Committee on Additive Manufacturing Technologies [8]. AM follows the popularisation of 3D solid modelling Computer Aided Design (CAD) [9].

Aerospace, automotive, biomedical and many other engineering fields benefit from the ability of AM to shape complex geometries with a high resolution and to customize the design for any needs (speeding up product development in automotive field [9], production of rough, engineered surface for more effective bone integration in medical field [10]).

In light of this, the present work proposes the use of a relatively new AM technique, Aerosol Jet Printing (AJP), to realize a customized measuring device with electrochemical sensors, addressable for the analysis of biological samples.

After an overview on the AJP method, the detailed materials and methods followed for device fabrication and testing will be described. Finally, preliminary results related to sensors geometrical and electrical features, together with an evaluation of the device compatibility with diagnostic assay routine for protein detection will be presented and discussed.

1.2 AJP: introduction and functioning principle

AJP is a quite novel additive manufacturing technique belonging to the family of Aerosol-based direct-write (A-DW), subset of droplet-based direct-write. It is also known as M^3D (maskless mesoscale materials deposition) and it was developed by Optomec under the Defense Advanced Research Projects Agency (DARPA) Mesoscopic Integrated Conformal Electronics (MICE) program. AJP functioning principle presents an aerosol beam directed toward a substrate to realize specific surface features (e.g., dots or lines) without using masks or post-patterning (i.e., laser trimming) [11].

The overall process is characterized by four steps: i) atomization of the ink, ii) densification of the generated aerosol, iii) focusing of the aerosol, iv) deposition of the droplets on the substrate [12].

Using a carrier gas (nitrogen or compressed dry air), a pneumatic Collison atomizer produces the aerosol starting from inks or dispersions with viscosities in a range between 1 and 1000 mPa·s. Following, a virtual impactor allows the carrier gas to be removed and the aerosol droplet size distribution to be adjusted. The typical setup allows the production of droplets smaller than 5 μm in diameter. The aerosol is focused in the print head, thanks to a sheath gas surrounding cylindrically the flow. The complex is accelerated when entering the print nozzle, thus to reach at the nozzle exit an inner radius inferior than 50 mm. Increasing the sheath gas flow additionally, the aerosol diameter can be reduced. The droplets, thanks to their high momentum, do not change their own direction, following the gas flow at the sample surface, and impact the substrate (two to five millimeters below the nozzle exit, with the surface perpendicular to it). The substrate could be heated to evaporate deposited solvents present inside the starting ink.

The performances obtained with commercially available system, able to print traces from 10 μm to 5mm in width at translation speeds up to 200 mm/s with a wide range of inks allowed to successfully use this technique for advanced applications, ranging from energy harvesting and flexible electronics to devices for bio-electronics applications. [13].

2 Materials and methods

2.1 Sensors design and fabrication

After evaluating commercially available and literature designs [14], sensors final layout was defined, using the 3-electrodes system (working (WE), counter (CE) and reference (RE) electrodes) commonly adopted for electrochemical measurements. The geometry was realized using AutoCAD, complete with a custom gadget by Optomec to ensure a proper ink filling. Figure 1 shows all the layers corresponding to the different employed inks: silver (in yellow) for the conductive tracks, carbon (in black) for WE and CE, silver chloride (in white) for RE and polyimide (in orange) for creating a sort of delimiting wall to help containing water-based samples. The selected geometry was reproduced on the substrate four times scaled in different dimensions, with a diameter of WE of 4 mm, 3 mm, 2 mm and 1mm respectively, with three sensors for each geometry to obtain a good repeatability (Fig. 1). Considerable attention was put in selecting the proper thickness of the lines and the distances between them, so that, tuning printer parameters according to ink viscosity, a homogeneous filling of the electrodes and pads could be ensured. The general design proposed might be customized through a proper functionalization with biomolecules that will ensure the specificity for the target analyte.

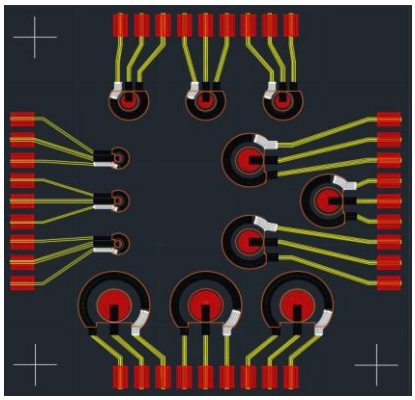

Fig. 1. AutoCAD drawing of the final prototype.

Alumina substrates were selected due to its mechanical properties and porosity, which ensures a proper ink adhesion. Regarding inks, the employed materials are: silver (UTDots Inc., cured at 220°C per 10 minutes) for conductive tracks, silver chloride (Fujikura Kasei. Co. Ltd., cured at 120°C per 30 minutes) for RE, carbon (Creative Materials Inc., cured at 115°C per 5 minutes) for WE and CE and polyimide (HD MicroSystems Inc., cured at 120°C per 20 minutes) for the final insulating layer.

Each ink was properly tuned with its own thinner to reach the proper viscosity and these two parts were placed in our Optomec's AJ300 printing machine, considering its own specific process parameters (table 1), in order to realize the final sensor presented in fig. 2a.

Table 1. Printing process parameters.

Process parameters	Ag	AgCl	C	PI
Sheath gas flow (SCCM)	50	130	40	150
Exhaust flow (SCCM)	830	600	1000	1300
Atomizer flow (SCCM)	810	550	900	1270
Process speed (mms-1)	2	2	2	3
Plate temperature (°C)	60	65	75	70

Further, in order to optimize liquid management. 3D wells were realized on each sensor by gluing on them glass-fiber washers.

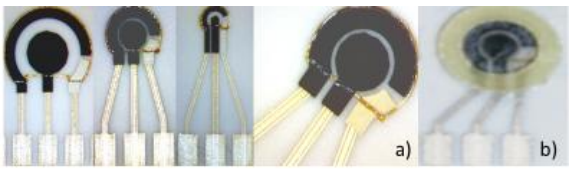

Fig. 2. a) Examples of the printed sensors on the alumina substrate, from left to right: 4 mm,3 mm,1 mm and 2 mm geometries; b) printed circuits with glued glass-fiber washers.

2.2 Sensors testing

In order to ensure the possibility to use the fabricated AJP sensors in experiments for proteins detection in biological samples, different features of the sensors were investigated.

First of all, a geometrical analysis was performed, in order to determine the thickness of printed lines for each type of ink and, for the overall circuit, to know the total area covered by the paths. The total area was evaluated as a sum of consecutive trapezoid areas.

A diamond stylus-based profilometer was used for step height measurements, (Alpha-Step IQ Kla Tencor) with a range 8 nm – 2 mm and an uncertainty of 0.1%. The system is provided of an integrated optical microscope which allows an automatized selection of the region of interest. The stylus speed can be tuned between 2 and 200 μm/s. The bending radius (nominal) of the diamond tip is 5 μm. Data are recorded and can be analyzed in real time by a dedicated software.

For sensors analysis, a testing force of 62×10^{-6} N was considered, together with the following process parameters:

- Scan speed: 50 μms^{-1} for PI, 20 μms^{-1} for Ag, AgCl and C;
- Scan length: 1000 μm;
- Sampling rate: 50 Hz.

Electrical resistance of the printed paths was measured using a digital bench-top multimeter (Hewlett-Packard 34401a), applying a testing probe to each extremity of each path, thus measuring the resistance offered by all its length. Both the resistance of sample geometries of pure inks and of each electrode of the complete sensors were measured. This allowed to compare resistivity values of each ink's datasheet with the ones obtained during tests and to evaluate the contribute of each material in the complete sensor. For each element, ten measures were performed, calculating then mean values and standard deviations.

Once these values were obtained, it was possible to get resistivity considering the definition of resistance:

$$R=\rho \cdot l \cdot S^{-1} \quad (1)$$

R is resistance, ρ is resistivity, l is the length of the considered path and S its section.

After completing the geometrical and electrical analysis, the optimal volumes (measured as amount of liquid, in μl), for each geometry, were defined depositing on each sensor using a micropipette different volumes of Phosphate Buffered Saline (PBS) (Sigma Aldrich) to optimize the values for future tests with biological samples. This test involved previously only the WE, to optimize the amount of volume for each step of the biofunctionalization, and then all three electrodes, to optimize the optimal volume for the final measurement.

After optimizing working volumes, the effectiveness of primary antibodies coating on the carbon WE was evaluated using a near infra-red imaging system (Odyssey® Fc Dual-Mode Imaging System from LI-COR Biosciences). More specifically, biomolecules adhesion onto carbon WE were qualitatively detected by labelling each antibody

with a fluorescent tag, and then recording the emitted light in the near infrared region using the Odyssey intensity quantifier.

A coating with an 8 µl/ml solution of anti-interleukin 8 primary antibody (Duo Set kit) was performed, keeping two electrodes as control (blank samples), covered with pure PBS solution. After that, sensors were placed in a humid chamber prepared through a box and wet paper to avoid solution evaporation and incubated for a night at 4 °C.

The next day, after washing with a solution of PBS with 0.05% Tween, sensors were incubated with a solution of secondary antibodies, labelled with a fluorescent tag functional for the final imaging. After two hours, sensors were washed and excited with a 685 nm light source, thus measuring the emitted light in the near infrared region with the Odyssey LI-COR system, in order to reveal the coating deposition.

Finally, a voltammetry based protein quantification was performed, using standard solutions of Interleukin 8 (IL-8), a member of the CXC chemokine subfamily, considered as universal biomarkers - from cancer and inflammation to neurodegeneration [15] - thus generalizing the use of the present PoC platform to various clinical fields. IL-8 strong interaction with its capture antibody, allows to reduce the variability to the functionalization phase. The protocol adopted for IL-8 quantification in this calibration phase of the circuit was characterized by a specific functionalization of the sensor using immunocomplexes formed by a capture and a detection antibody, using a dedicated kit (DuoSet development system for ELISA, Human CXCL8/IL-8), and by an Anodic Stripping Voltammetry (ASV) based measurement technique, optimized in [16], [17].

All electrodes were exposed to the same bio-functionalization steps as following: i) overnight immobilization of IL-8 antibody to sensor surfaces via drop-casting; ii) 2-hours incubation with IL-8 sample (10 ng/ml); iii) 2 hours incubation with biotin-labelled detection antibody; iv) addition of streptavidine-tagged Alkaline Phosphatase (AP) enzyme that catalyzes the oxidation of ionic Ag ($AgNO_3$) to metallic Ag, thanks to the reaction happening in presence of Ascorbic acid (AA-p), as described in [18].

Once completing the bio-functionalization, sensors were covered with optimized measurement volumes of PBS, a constant potential of -0.12 V was applied for 10 s and then a linear sweep voltammetry was performed at a scan rate of 40 mV/s up to +0.4 V, measuring Ag oxidation current. All measurements were performed using a potentiostat (Palmsens, Compact Electrochemical Interfaces) controlled using the devoted software.

3 Results

3.1 Geometrical analysis

Results obtained from the geometrical analysis (Table 2) showed congruent thicknesses of all the path with the nominal values stated in the datasheet of the Optomec Printing System (single layer thickness in the range 100 nm to 10 µm). The differences between the results obtained for each ink can be interpreted and compared taking into account different process parameters, number of printed layers and further considering viscosity: higher thicknesses were obtained for inks with higher viscosity.

Table 2. Thickness and sections of deposited inks.

Material	Thickness (μm)	Standard Deviation	Section (μm^2)
Ag	6.8	±1	854.2
AgCl	4	±1	392.3
C	6.5	±0.2	365.3
PI	2.7	±2	/

3.2 Electrical analysis

Data presented in table 3 appeared in agreement with the nominal values of the manufacturers, taking into account the specific process parameters.

More in detail, Ag experimental resistivity ($12{,}2 \cdot 10^{8}$ Ωm) can be compared with the nominal one ($3 \cdot 10^{-8}$ Ωm), considering as most relevant affecting variables the substrate (ceramic is not included among the optimal indicated by UTDots). AgCl experimental resistivity value ($71{,}3 \cdot 10^{-8}$ Ωm) can be compared with the nominal one reported by Fujikura Kasei. Co. Ltd ($56 \cdot 10^{-8}$ Ωm), considering the use of the thinner to achieve the viscosity required for printing. Finally, C experimental resistivity ($159{,}6 \cdot 10^{-8}$ Ωm) appear increased compared to the theorical one given by Creative Materials ($15.5 \cdot 10^{-8}$ Ωm), probably due to the usage of a non-optimal substrate and due to different post-processing parameters. Measurements performed on the complete sensors suggested values of resistance coherent with the different dimensions of each geometry, with standard deviation suggesting a good reproducibility of the purposed technique for printing the same geometry.

Table 3. Resistance and resistivity of deposited inks.

Material	Resistance (Ω)	Path Length (mm)	Resistivity (Ωm)
Ag	4.9	13.5	$30.8 \cdot 10^{-8}$
	1.6	11	$12.2 \cdot 10^{-8}$
	7.3	9.5	$65.8 \cdot 10^{-8}$
AgCl	21	12	$71.3 \cdot 10^{-8}$
	19.1	10	$78.2 \cdot 10^{-8}$
	25.3	11.5	$89.8 \cdot 10^{-8}$
C	67.5	13	$122.9 \cdot 10^{-8}$
	39.9	13	$72.6 \cdot 10^{-8}$
	84.3	12.5	$159.6 \cdot 10^{-8}$

3.3 Fluorescence imaging

Results shown in Fig. 3 highlight a significant difference between blank electrodes (black in the image, not emitting any light) and antibodies coated ones (appearing as a clearer emitting spot in the image). The red arrow indicates the zone successfully covered by antibodies.

These findings confirmed the possibility to use these materials and AJP technique to produce electrodes, which allow a homogeneous adhesion of antibodies, essential to perform a complete functionalization to perform immune-sensing of proteins. The homogeneous deposition of primary antibodies would allow a more effective quantification of proteins, thus reducing the interference of currents due to un-specific adsorption.

Fig. 3. Three alumina-substrate sensors covered by protein.

3.4 Protein quantification

Significant differences in term of peak height could be appreciated comparing results from sensors tested with protein solution and blank ones. This suggests the possibility to successfully apply the described ASV protocol for protein quantification on all the AJP sensors (fig. 4).

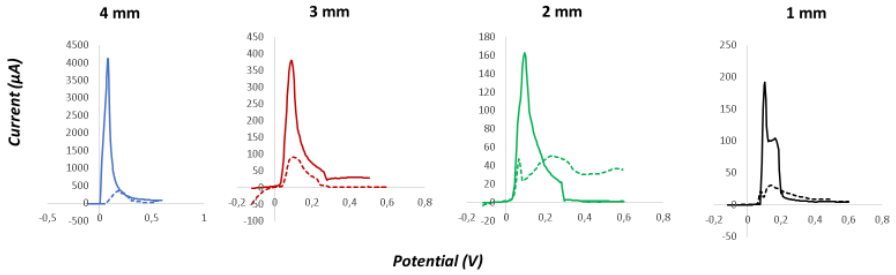

Fig. 4. Plots obtained during protein quantification test for the alumina substrate sensor; each plot measures current (expressed in µA) as a function of potential (expressed in V). Dotted lines represent "blank samples".

The higher difference could be recorded for sensors with 4 mm WE, reproducing the geometry of products already available on the market. However, very interesting results could be obtained with the smaller geometries. The results obtained for the other two intermediate geometries on alumina can be considered comparable. Even if the normalized current peak is significantly smaller than the one obtained with the other geometries, they can be considered as a of good compromise considering all the electronic and the biological specific requirements.

Regarding 1 mm geometry, the current peak obtained (~200µA) is very high, considering the significantly smaller area, and it is probably due to the closeness of the electrodes that allow virtually all current to be "captured" and little to be lost. The negative aspect related to this geometry is connected to the biological aspect, considering future applications for the detection of disease-related biomarkers of present in a very

low concentration (< ng/ml) for which in 2 µl of sample (the one required for this smallest geometry) there is a high risk not to deposit any protein on sensor WE.

4 Conclusions

3D printing technologies are increasingly emerging as potential tool to bring significant improvements in the medical and biotechnological fields. Further the possibility to print with high resolution conductive materials open a wide variety of possibilities for producing all the sensors that are involved in bio-electronics applications.

In this picture, this work reports the realization of a microsensor platform for protein detection, using a new 3D printing technique: Aerosol Jet Printing.

Results obtained from geometrical and electrical tests suggested that the lines realized via AJP are microscopic with controllable thickness and with proper values of electrical resistivity coherent with each ink. Furthermore, imaging findings confirmed good adhesion of antibodies on sensors WE and to both the employed substrates. ASV measurements confirmed the possibility to use the sensors for quantifying protein in a sample (10ng/ml).

In light of this, future studies will test the capability of the sensors to trace the presence of proteins in different biological fluids. To achieve this goal, future developments will address complete calibrations of the platform for protein detection, taking into account all the interferences that might be introduced from the chemistry of real samples (e.g. blood, plasma).

Furthermore, future development might address techniques for improving the confinement of liquid samples both for WE functionalization and for the final measurement, using biocompatible soft materials, (e.g. PDMS). Through a proper modification of the sensor geometry presented and the usage of proper inks, AJP technology would allow the possibility to integrate the electrodes on a customized substrate with 3D wells. Overall, the sensors might be properly integrated with dedicated conditioning electronics and microfluidic, in order to optimize both the electronic performances and liquid samples managing.

References

1. A. Spanu, S. Lai, P. Cosseddu, M. Tedesco, S. Martinoia, and A. Bonfiglio, “An organic transistor-based system for reference-less electrophysiological monitoring of excitable cells,” *Sci. Rep.*, vol. 5, no. 1, p. 8807, 2015.
2. R. A. S. Couto, J. L. F. C. Lima, and M. B. Quinaz, “Recent developments, characteristics and potential applications of screen-printed electrodes in pharmaceutical and biological analysis,” *Talanta*, vol. 146, no. 228, pp. 801–814, 2016.
3. J. Li, F. Rossignol, and J. Macdonald, “Inkjet printing for biosensor fabrication: combining chemistry and technology for advanced manufacturing,” *Lab Chip*, vol. 15, no. 12, pp. 2538–2558, 2015.
4. W. Kit-Anan *et al.*, “Disposable paper-based electrochemical sensor utilizing inkjet-printed Polyaniline modified screen-printed carbon electrode for Ascorbic acid

detection," *J. Electroanal. Chem.*, vol. 685, pp. 72–78, 2012.

5. C. Hu, X. Bai, Y. Wang, W. Jin, X. Zhang, and S. Hu, "Inkjet printing of nanoporous gold electrode arrays on cellulose membranes for high-sensitive paper-like electrochemical oxygen sensors using ionic liquid electrolytes," *Anal. Chem.*, vol. 84, no. 8, pp. 3745–3750, 2012.
6. H. Ragones *et al.*, "Disposable electrochemical sensor prepared using 3D printing for cell and tissue diagnostics," *Sensors Actuators, B Chem.*, vol. 216, pp. 434–442, 2015.
7. H. Yang, T. Rahman, D. Du, R. Panat, and Y. Lin, "3-D Printed Adjustable Microelectrode Arrays for Electrochemical Sensing and Biosensing.," *Sens. Actuators. B. Chem.*, vol. 230, pp. 600–606, Jul. 2016.
8. *Wohlers Report 2015, 3D Printing and Additive Manufacturing State of the Industry, Annual Worldwide Progress Report.* 2015.
9. I. Gibson, "The changing face of additive manufacturing," *J. Manuf. Technol. Manag.*, vol. 28, no. 1, pp. 10–17, 2017.
10. N. Guo and M. C. Leu, "Additive manufacturing: Technology, applications and research needs," *Front. Mech. Eng.*, vol. 8, no. 3, pp. 215–243, 2013.
11. J. M. Hoey, A. Lutfurakhmanov, D. L. Schulz, and I. S. Akhatov, "A review on aerosol-based direct-write and its applications for microelectronics," *J. Nanotechnol.*, vol. 2012, 2012.
12. S. Binder, M. Glatthaar, and E. Rädlein, "Analytical investigation of aerosol jet printing," *Aerosol Sci. Technol.*, vol. 48, no. 9, pp. 924–929, 2014.
13. OPTOMEC, "Aerosol Jet ® Printed Electronics Overview," p. 6.
14. C. S. Alex Gong, W. J. Syu, K. F. Lei, and Y. S. Hwang, "Development of a flexible non-metal electrode for cell stimulation and recording," *Sensors (Switzerland)*, vol. 16, no. 10, 2016.
15. H. J. Kim, H. Li, J. J. Collins, D. E. Ingber, D. J. Beebe, and R. F. Ismagilov, "Contributions of microbiome and mechanical deformation to intestinal bacterial overgrowth and inflammation in a human gut-on-a-chip," *Pnas*, no. 13, pp. E7–E15, 2015.
16. S. Tonello *et al.*, "Wireless Point-of-Care Platform with Screen-Printed Sensors for Biomarkers Detection," *IEEE Trans. Instrum. Meas.*, vol. 66, no. 9, 2017.
17. S. Tonello *et al.*, "Enhanced sensing of interleukin 8 by stripping voltammetry: Carbon nanotubes versus fullerene," in *IFMBE Proceedings*, 2017, vol. 65.
18. Z. P. Chen, Z. F. Peng, J. H. Jiang, X. B. Zhang, G. L. Shen, and R. Q. Yu, "An electrochemical amplification immunoassay using biocatalytic metal deposition coupled with anodic stripping voltammetric detection," *Sensors Actuators, B Chem.*, vol. 129, no. 1, pp. 146–151, 2008.